

Article

N-O Ligand Supported Stannylenes: Preparation, Crystal, and Molecular Structures

Hannah S. I. Sullivan^{1,2}, Andrew J. Straiton¹ , Gabriele Kociok-Köhn³ and Andrew L. Johnson^{1,*} ¹ Department of Chemistry, University of Bath, Bath BA2 7AY, UK² Centre for Sustainable Chemical Technologies, University of Bath, Bath BA2 7AY, UK³ Material and Chemical Characterisation Facility (MC²), University of Bath, Bath BA2 7AY, UK

* Correspondence: a.l.johnson@bath.ac.uk

Abstract: A new series of tin(II) complexes (**1**, **2**, **4**, and **5**) were successfully synthesized by employing hydroxy functionalized pyridine ligands, specifically 2-hydroxypyridine (hpH), 8-hydroxyquinoline (hqH), and 10-hydroxybenzo[h]quinoline (hbqH) as stabilizing ligands. Complexes [Sn(μ - κ^2 ON-OC₅H₄N)(N{SiMe₃})₂]₂ (**1**) and [Sn₄(μ - κ^2 ON-OC₅H₄N)₆(κ^1 O-OC₅H₄N)₂] (**2**) are the first structurally characterized examples of tin(II) oxypyridinato complexes exhibiting {Sn₂(OCN)₂} heterocyclic cores. As part of our study, ¹H DOSY NMR experiments were undertaken using an external calibration curve (ECC) approach, with temperature-independent normalized diffusion coefficients, to determine the nature of oligomerisation of **2** in solution. An experimentally determined diffusion coefficient (298 K) of $6.87 \times 10^{-10} \text{ m}^2 \text{ s}^{-1}$ corresponds to a hydrodynamic radius of Ca. 4.95 Å. This is consistent with the observation of an averaged hydrodynamic radii and equilibria between dimeric [Sn{hp}]₂ and tetrameric [Sn{hp}]₄ species at 298 K. Testing this hypothesis, ¹H DOSY NMR experiments were undertaken at regular intervals between 298 K–348 K and show a clear change in the calculated hydrodynamic radii from 4.95 Å (298 K) to 4.35 Å (348 K) consistent with a tetramer \rightleftharpoons dimer equilibria which lies towards the dimeric species at higher temperatures. Using these data, thermodynamic parameters for the equilibrium ($\Delta H^\circ = 70.4 (\pm 9.22) \text{ kJ mol}^{-1}$, $\Delta S^\circ = 259 (\pm 29.5) \text{ J K}^{-1} \text{ mol}^{-1}$ and $\Delta G^\circ_{298} = -6.97 (\pm 12.7) \text{ kJ mol}^{-1}$) were calculated. In the course of our studies, the Sn(II) oxo cluster, [Sn₆(m³-O)₆(OR)₄:{Sn(II)(OR)₂}]₂ (**3**) (R = C₅H₄N) was serendipitously isolated, and its molecular structure was determined by single-crystal X-ray diffraction analysis. However, attempts to characterise the complex by multinuclear NMR spectroscopy were thwarted by solubility issues, and attempts to synthesise **3** on a larger scale were unsuccessful. In contrast to the oligomeric structures observed for **1** and **2**, single-crystal X-ray diffraction studies unambiguously establish the monomeric 4-coordinate solid-state structures of [Sn(κ^2 ON-OC₉H₆N)₂] (**4**) and [Sn(κ^2 ON-OC₁₃H₈N)₂] (**5**).



Citation: Sullivan, H.S.I.; Straiton, A.J.; Kociok-Köhn, G.; Johnson, A.L. N-O Ligand Supported Stannylenes: Preparation, Crystal, and Molecular Structures. *Inorganics* **2022**, *10*, 129. <https://doi.org/10.3390/inorganics10090129>

Academic Editors: Simon Aldridge and Stephen Mansell

Received: 26 July 2022

Accepted: 20 August 2022

Published: 31 August 2022

Publisher's Note: MDPI stays neutral with regard to jurisdictional claims in published maps and institutional affiliations.



Copyright: © 2022 by the authors. Licensee MDPI, Basel, Switzerland. This article is an open access article distributed under the terms and conditions of the Creative Commons Attribution (CC BY) license (<https://creativecommons.org/licenses/by/4.0/>).

Keywords: stannylene; 2-hydroxy-pyridine; 8-hydroxyquinoline; 10-hydroxybenzo[h]quinoline; molecular structures; DOSY NMR

1. Introduction

The chemistry of heavy carbene analogues [MR₂:M = Si, Ge, Sn, Pb; R = stabilizing anionic ligand) has attracted considerable interest for some time now and is of fundamental interest in main group p-block chemistry [1–3]. Their marked dual Lewis acidic and Lewis basic characteristics, alongside steric and electronic tuneability via astute ligand selection result in diverse and often unique chemistry [2].

A particular class of tetrylenes of interest are the stannylene complexes with the general formula [Sn(R-L)_{2-x}(X)_x], where [R-L] is a monoanionic ligand bearing a lariat donor group (L) fragment capable of forming either intra- or inter-molecular Lewis base adducts with the metal atom, Figure 1, thus acting as an anionic chelate or bridging ligand, and where X is an ancillary monodentate ligand such as a halogen atom or {N(SiMe₃)₂} group [4–9]. These Sn(II) compounds have potential applications as ligands for transition

metals, intermediates in organic synthesis [10–13], catalysts in the conversion of small molecules [14–20] or the ring opening polymerisation of lactones [21], or as precursors for electronic thin film materials [8,18,22–26].

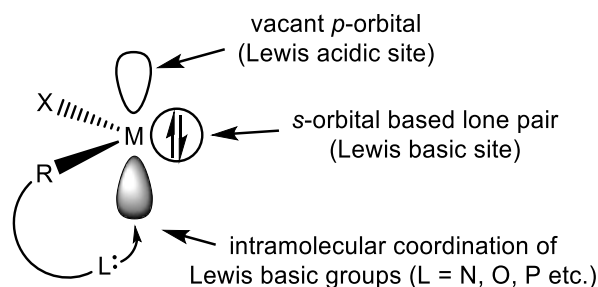
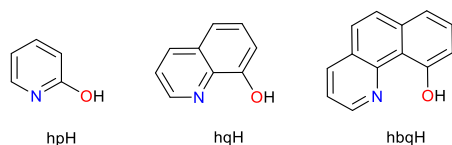


Figure 1. Stabilization of stannylene $[\text{Sn}(\text{R-L})_{2-x}(\text{X})_x]$ complexes.

It is well established that the nature of the ligand (donor atoms) has a significant effect on the chemical and structural properties of these heavy carbene analogues. Amongst the library of $[\text{Sn}(\text{II})(\text{R-L})_{2-x}(\text{X})_x]$ systems, perhaps the most frequently studied are those bearing an $\text{N-N}'$ chelate as the $[\text{R-L}]$ ligands, such as amidinates [22,27–29], guanidinates [8,25,30–33], β -diketiminates [5,21,34–39], and amino/imino-pyrrolides [9]. While $\text{Sn}(\text{II})$ $[\text{Sn}(\text{R-L})_{2-x}(\text{X})_x]$ systems bearing an N,O chelate ligand such as amino alcohols [7,40–48], amino-phenols [49], organic amides [23,50], salicylaldiminato [50–53], ketiminate [54], and hydroxyquinolinates [55–64] are known, their derivative chemistry is less developed.

While the anionic derivatives of 2-hydroxypyridine (hpH) [65,66] and 8-hydroxyquinoline (hqH) [67,68] have been utilized as 1,3- 1,4- $\kappa^2\text{N,O}$ chelate ligands, respectively, for a range of metals, examples of the coordination chemistry of 10-hydroxybenzo[h]quinoline (hbqH) (Figure 2) and its derivatives are scarce, despite its commercial availability.

(A) 1,3- N,O , 1,4- N,O and 1,5- N,O Chelate ligands



(B) Oxypyridinato ligand Coordination modes

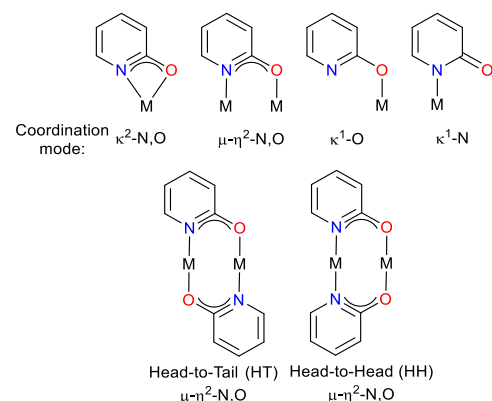


Figure 2. Overview of the N,O donor pro-ligands, hpH, hqH, and hbqH used in this study (A), and the common coordination modes observed for the 2-hydroxypyridinato (hp) ligand (B).

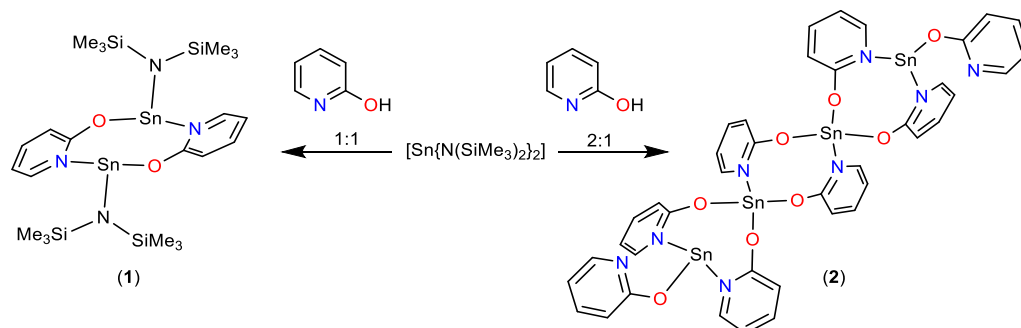
The anions of 2-hydroxypyridine derivatives belong to a wider class of tri-atomic bridging ligands, such as carboxylate, triazenide, amidinate, sulfonates, and phosphates [65,69]. The presence of two different donor atoms results in rich coordination chemistry with a variety of potential binding modes for the oxypyridinato ligand, common examples of which are shown in Figure 2, illustrating the unusual binding modes of the $\{\text{hp}\}$ ligand

that constrained 1,3-*N,O* (four-membered ring) coordination can induce. A search of the literature reveals numerous oxypyridinato ligated transition metal complexes, whilst there are in comparison only a handful of main group complexes (reported in the CSD) [70–75], and to date, none of these represent Sn(II)-supported species. In contrast, the quinolinato, {hq} and the oxybenzo[h]quinolinato {hbq} ligands exclusively display 1,4- and 1,5- κ^2 -*N,O* coordination modes, respectively.

To-date, Sn(II) derivatives of these systems (i.e., {hp}, {hq} and {hbq}), are limited to a handful of homoleptic [61,64] and heteroleptic [55–60,62,63] Sn(II) hydroxyquinolate complexes. Here, we describe the details of the synthesis and structure of a series of Sn(II) complexes supported by the 1,3-, 1,4- and 1,5- κ^2 -*N,O* chelate ligands oxypyridinato (hpH), hydroxyquinolinato {hqH} and oxybenzo[h]quinolinato {hbq}, respectively.

2. Synthesis of Tin(II) Complexes

In all cases, the isolated products were characterised by solution-state NMR (^1H , $^{13}\text{C}\{^1\text{H}\}$ and $^{119}\text{Sn}\{^1\text{H}\}$) spectroscopy and elemental analysis. The reaction of the bulky Sn(II) amide system $[\text{Sn}\{\text{N}(\text{SiMe}_3)_2\}_2]$ with ligand 2-hydroxypyridine in a stoichiometric 1:1 reaction results in the formation and isolation after recrystallisation (-28°C in toluene), of complex **1** as pale yellow crystals (Scheme 1). The ^1H NMR spectrum of **1** (in C_6D_6) clearly shows the presence of a singlet resonance at $\delta = 0.37$ ppm, representative of the presence of an {HMDS} group. The ^1H NMR spectra also clearly show a series of four multiplets corresponding to the aromatic protons of the {hp} ligand at $\delta = 6.20, 6.48, 6.97$ and 7.99 ppm, respectively, in a 1:1:1:18 ratio, with the $\{\text{N}(\text{SiMe}_3)_2\}$ group indicating the formation of a mono-substituted complex of the general form $[\{\text{hp}\}\text{Sn}\{\text{N}(\text{SiMe}_3)_2\}]$. This is supported by the $^{13}\text{C}\{^1\text{H}\}$ NMR spectra, which clearly show the expected six resonances [$\delta = 170.0, 142.6, 142.2, 116.6, 114.0,$ and 5.9 ppm].



Scheme 1. Formation of complexes **1** and **2**.

Likewise, the $^{119}\text{Sn}\{^1\text{H}\}$ NMR spectra shows a single sharp resonance [$\delta = -84.9$ ppm], respectively, (cf. $\delta = 776.0$ ppm, for $[\text{Sn}\{\text{N}(\text{SiMe}_3)_2\}_2]$). A reaction of $[\text{Sn}\{\text{N}(\text{SiMe}_3)_2\}_2]$ with two equivalents of 2-hydroxypyridine in toluene results in the formation of a colourless precipitate, which, after heating into solution followed by filtration and cooling, afforded a crop of colourless crystals of **2**. The ^1H NMR spectrum of **2** (in C_6D_6) shows only four multiplets corresponding to the aromatic protons of the {hp} ligand at $\delta = 6.02, 6.62, 6.92,$ and 7.63 ppm, respectively, in a 1:1:1:1 ratio. The clear absence of a peak corresponding to the $\{\text{N}(\text{SiMe}_3)_2\}$ group indicates the formation of a *bis*-substituted complex of the general form $[\text{Sn}\{\text{hp}\}_2]$. The ^{13}C NMR spectra consist of five resonances [$\delta = 112.7, 115.7, 140.4, 143.7,$ and 169.3 ppm], while the ^{119}Sn NMR spectra display a single broad resonance at $\delta = -525.5$ ppm. Low-temperature NMR studies (223 K) on complex **2** in d_8 -Tol showed no significant changes in the ^1H , $^{13}\text{C}\{^1\text{H}\}$, or $^{119}\text{Sn}\{^1\text{H}\}$ NMR spectra, suggestive of an exchange process faster than the NMR time scale even at 223 K. Below 223 K, low solubility issues resulted in the loss of the ^{119}Sn signal.

To determine the nature of the oligomerisation of **2** in solution, ^1H DOSY NMR experiments were undertaken, using the novel external calibration curve (ECC) approach,

with temperature-independent normalized diffusion coefficients, for MW-determination described by Stalke et al. [76,77].

The room temperature (298 K) ^1H DOSY NMR spectrum for compound **2**, shown in Figure 3, clearly shows a single diffusion coefficient ($D_{\text{norm}} = 6.87 \times 10^{-10} \text{ m}^2 \text{ s}^{-1}$) which corresponds to a hydrodynamic radius of *Ca.* 4.95 Å.

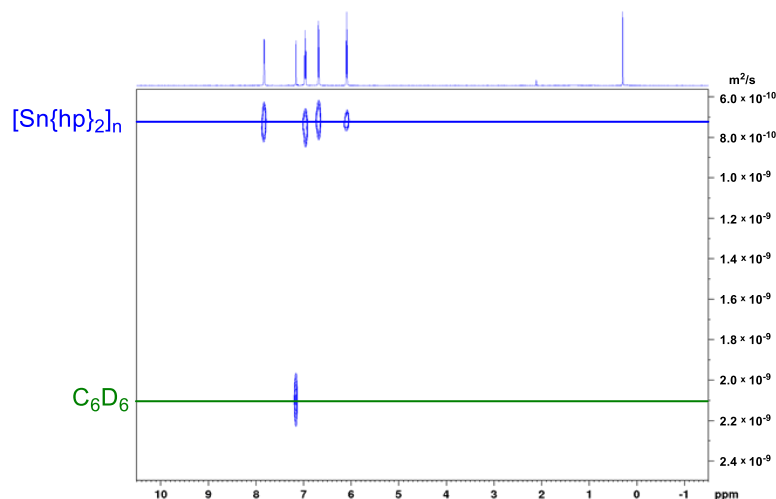
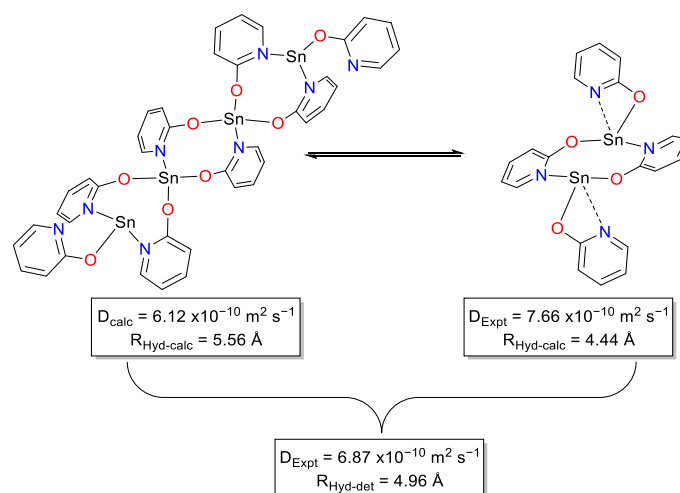


Figure 3. Plot showing the ^1H DOSY NMR spectrum for compound **2** (298 K).

Based on the single-crystal data (*infra vide*), the molecular volume of the tetrameric **2** observed in the solid state was calculated as *ca.* 721 \AA^3 , with a molecular radius of 5.56 \AA . While molecular shapes are important to the accurate interpretation of diffusion data, diffusion coefficient/molecular weight correlation studies have shown that merged calibration curves based around molecules in solution behave as either (i) compact spheres, (ii) dissipated spheres or ellipsoids, or (iii) expanded discs that can be used to estimate molecular weights.

Assuming each “[Sn{hp}₂]” unit is “spherical” and possesses an approximate volume of 183 \AA^3 , as determined by X-ray crystallography, the experimentally determined hydrodynamic volume, based on the Stokes-Einstein equation, is consistent with the presence of a trimeric species in solution. While a trimeric species is possible, we believe a more likely scenario is that the experimentally determined hydrodynamic volume is an averaged diffusion coefficient (and hydrodynamic volume) constant with a rapid (on the NMR timescale) equilibria between dimeric [Sn{hp}₂]₂ and tetrameric [Sn{hp}₂]₄ species (Scheme 2) at 296 K.



Scheme 2. Proposed Tetramer Dimer equilibria observed for **2**.

Using Stalke's method, and correcting empirically for molecular density (using an empirically determined density correction factor of 1.5535 and hence accounting for the heavy Sn atom) [78], we predict a molecular mass of 937 Da (*c.f.* a calculated mass for a trimeric species $[\text{Sn}\{\text{hp}\}_2]_3$ of 921 Da, 2% error). To test our hypothesis, ^1H DOSY NMR experiments were undertaken at regular intervals between 298 K–348 K. Table 1 and Figure 4 show the diffusion coefficients of **2**, 5.43 mM in *d*⁸-Tol as a function of temperature. At 298 K, ^1H DOSY NMR affords an experimentally determined diffusion coefficient of $D = 7.97 \times 10^{-10} \text{ m}^2 \text{ s}^{-1}$, which on warming to 348 K increases to $D = 1.75 \times 10^{-9} \text{ m}^2 \text{ s}^{-1}$. The observed change in the calculated hydrodynamic radii is concomitant with a decrease in the calculated hydrodynamic radii, such that at 348 K $R_{\text{Hyd-cal}} = 4.37 \text{ \AA}$ (*c.f.* $R_{\text{Hyd-cal}} = 4.93 \text{ \AA}$ at 298 K and a crystal graphically determined $R = 4.44 \text{ \AA}$) consistent with a tetramer \rightleftharpoons dimer equilibria which lies towards the dimeric species at higher temperatures. When cooled to room temperature, the observed diffusion coefficient returns to $D = 7.97 \times 10^{-10} \text{ m}^2 \text{ s}^{-1}$, implying a low barrier to tetramer formation.

Table 1. Experimentally determined (^1H DOSY NMR) diffusion coefficients (D), calculated Hydrodynamic radii ($R_{\text{Hyd-cal}}$) and calculated Molecular volume (V_{cal}) of **2** at temperatures between 298–348 K.

Temp (K)	$D \text{ (m}^2\text{s}^{-1}\text{)}$	$R_{\text{Hyd-cal}} \text{ (\AA)}$	$V_{\text{cal}} \text{ (\AA}^3\text{)}$
298	7.974×10^{-10}	4.93	503
308	9.416×10^{-10}	4.85	477
318	1.116×10^{-9}	4.70	436
328	1.310×10^{-9}	4.57	400
338	1.538×10^{-9}	4.41	360
348	1.750×10^{-9}	4.37	350

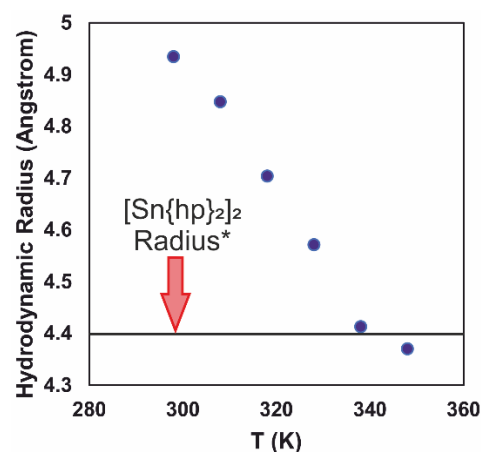


Figure 4. Graph showing the experimentally determined diffusion coefficients of **2**, 5.43 mM in *d*⁸-Tol, as a function of temperature. *: Radius (4.44 Å) as determined by single-crystal X-ray diffraction.

A subsequent attempt followed to obtain thermodynamic parameters for the equilibrium process from the experimentally observed diffusion coefficients and the crystal graphically determined radii of the tetramer and the dimer species, which in turn can be used to estimate the molar fractions of the tetramer and dimer in solution and the equilibrium constants K at various temperatures (see ESI). A plot of $\ln(K_{\text{eq}})$ vs. $1/T$ reveals an endothermic reaction process with the following parameters: $\Delta H^\circ = 70.4 (\pm 9.22) \text{ kJ mol}^{-1}$, $\Delta S^\circ = 259 (\pm 29.5) \text{ J K}^{-1} \text{ mol}^{-1}$, and $\Delta G^\circ_{298} = -6.97 (\pm 12.7) \text{ kJ mol}^{-1}$.

While these values are only estimates, and no substantial emphasis should be placed on them, the values may be compared with those found for another dimer–tetramer equilibrium process [79] and indicate that in this instance, tetramer formation is significantly favoured at lower temperatures.

3. Single-Crystal X-ray Diffraction Studies and Molecular Structures of Tin(II) Complexes

X-ray diffraction studies on single crystals of complexes **1**, **2**, **4**, and **5** unambiguously established their solid-state structures. The structures of the heteroleptic and homoleptic complexes, $[\text{Sn}(\mu\text{-}\kappa^2\text{ON-OC}_5\text{H}_4\text{N})(\text{N}\{\text{SiMe}_3\}_2)]_2$ (**1**), and $[\text{Sn}_4(\mu\text{-}\kappa^2\text{ON-OC}_5\text{H}_4\text{N})_6(\kappa^1\text{O-OC}_5\text{H}_4\text{N})_2]$ (**2**) are shown in Figures 5 and 6, respectively, with selected bond lengths and angles in Tables 2 and 3, respectively. Compound **1** (Figure 5) exists as a centrosymmetric dimer in the solid-state, comprising two independent $[\text{hp}\{\text{Sn}\{\text{N}(\text{SiMe}_3)_2\}]$ molecules in the asymmetric unit cell, with symmetry operators generating the second half of each dimer.

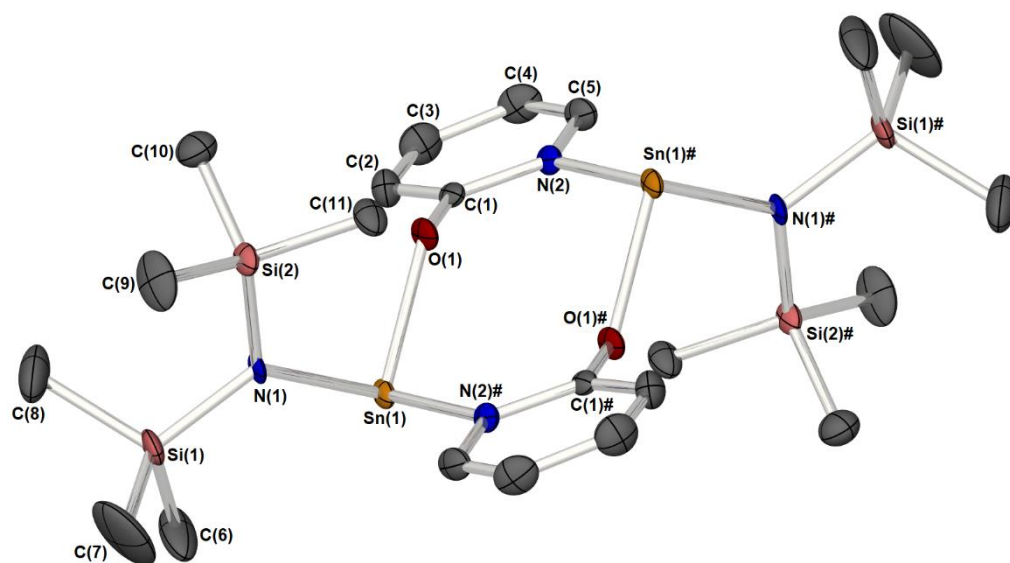


Figure 5. The molecular structure of one of the two full molecules of complex **1** present in the unit cell. Symmetry transformations (#) used to generate equivalent atoms; #: $-X$, $-Y$, $1-Z$. Thermal ellipsoids are shown at 50% probability. Hydrogen atoms have been omitted for clarity.

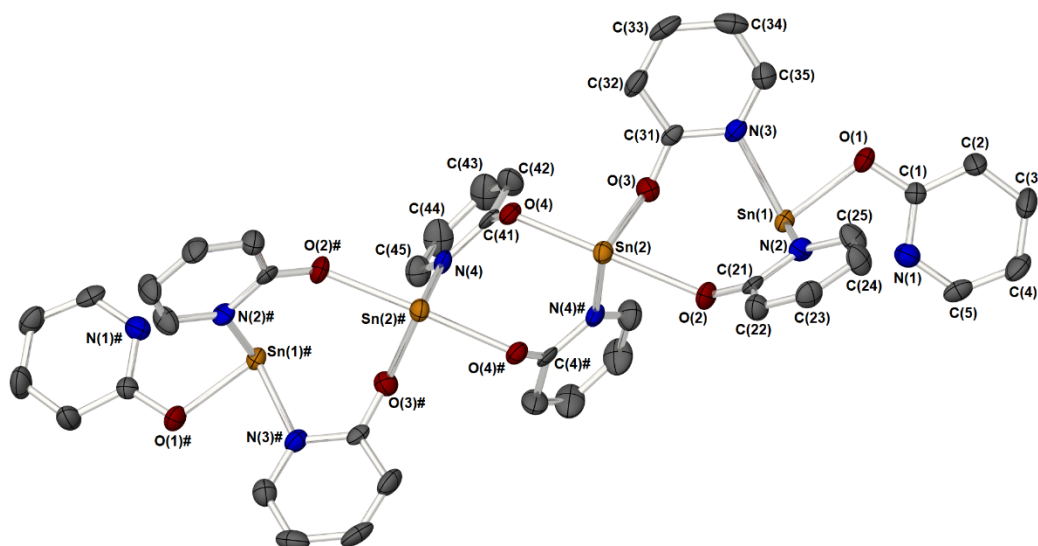


Figure 6. The solid-state molecular structure of complex **2**. Symmetry transformations (#) used to generate equivalent atoms; #: $3/2-X$, Y , $1-Z$. Thermal ellipsoids are shown at 50% probability. Hydrogen atoms have been omitted for clarity.

Table 2. Selected bond lengths (Å) and bond angles (°) for complex 1. Symmetry-generated atoms are marked with (#).

Selected Bond Lengths (Å)		Selected Bond Angles (°)	
Sn(1)-N(1)	2.1009(16)	N(1)-Sn(1)-N(2)#	90.30(7)
Sn(2)-N(3)	2.1064(16)	N(1)-Sn(1)-O(1)	93.36(6)
		O(1)-Sn(1)-N(2)#	90.72(6)
Sn(1)-O(1)	2.1491(14)		
Sn(2)-O(2)	2.1434(15)	N(3)-Sn(2)-N(4)#	90.08(7)
		N(3)-Sn(2)-O(2)	92.91(6)
Sn(1)-N(2)	2.2751(19)	O(2)-Sn(2)-N(4)#	92.46(6)
Sn(2)-N(4)	2.2590(19)		
C(1)-O(1)	1.302(3)	O(1)-C(1)-N(2)	116.7(2)
C(1)-N(2)	1.355(3)	O(2)-C(21)-N(4)	116.6(2)
C(21)-O(2)	1.302(3)		
C(21)-N(4)	1.351(3)	O(1)-C(1)-N(2)-Sn(1)#	3.2(2)
		O(2)-C(21)-N(4)-Sn(2)#	3.0(2)

Table 3. Selected bond lengths (Å) and bond angles (°) for complex 2. Symmetry-generated atoms are marked with (#).

Selected Bond Lengths (Å)		Selected Bond Angles (°)	
Sn(1)-O(1)	2.135(3)	N(2)-Sn(1)-N(3)	86.64(13)
Sn(1)-N(2)	2.239(4)	O(1)-Sn(1)-N(2)	87.04(14)
Sn(1)-N(3)	2.337(4)	O(1)-Sn(1)-N(3)	79.58(13)
Sn(2)-O(2)	2.370(3)	O(2)-Sn(2)-O(4)	157.89(13)
Sn(2)-O(3)	2.142(3)	O(3)-Sn(2)-N(4)#	83.40(14)
Sn(2)-O(4)	2.263(3)	O(2)-Sn(2)-O(3)	78.57(12)
Sn(2)-N(4)#	2.230(4)	O(2)-Sn(2)-N(4)#	78.58(13)
		O(3)-Sn(2)-O(4)	86.85(12)
O(1)-C(1)	1.322(5)	O(4)-Sn(2)-N(4)#	83.35(12)
C(1)-N(1)	1.333(6)	O(1)-C(1)-N(1)	116.5(4)
O(2)-C(21)	1.289(6)	O(2)-C(21)-N(2)	116.1(4)
C(21)-N(2)	1.357(6)	O(3)-C(31)-N(3)	116.6(4)
O(3)-C(31)	1.310(6)	O(4)-C(41)-N(4)	116.4(4)
C(31)-N(3)	1.347(6)	Sn(1)-O(1)-C(1)-N(1)	6.8(5)
O(4)-C(41)	1.297(6)	Sn(1)-N(2)-C(21)-O(2)	0.6(5)
C(41)-N(4)	1.348(6)	Sn(1)-N(3)-C(31)-O(3)	2.3(5)
		Sn(2)#-N(4)-C(41)-O(4)	0.4(4)

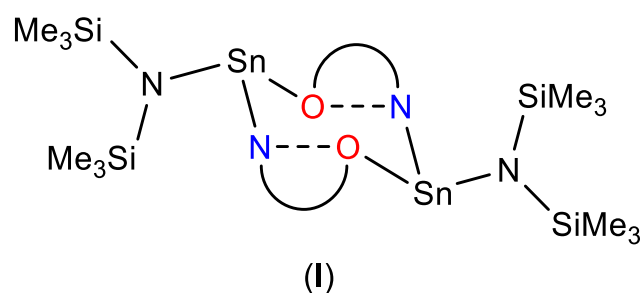
Both the oxygen and nitrogen donor atoms of the oxypyridinato ligands bridge the two *transoidal* Sn{N(SiMe₃)₂} moieties in a head-to-tail (HT) μ - η^2 coordination mode, resulting in an eight-membered Sn₂O₂C₂N₂ cyclic core to the molecule.

Each Sn(II) centre in **1** is three-coordinate and may be regarded as being at the centre of a distorted trigonal pyramid in which the Sn atoms are coordinated by one oxygen atom and one nitrogen atom from two different {hp} ligands in a “Head-to-Tail” fashion (see Figure 2), as well as the nitrogen of a terminal {N(SiMe₃)₂} ligand [Sn(1)-N(1) 2.101(2) Å and Sn(2)-N(3) 2.106(2) Å]. The bond angles about each Sn(II) atom in **1** [i.e., N(2A)-Sn(1)-O(1) 90.71°; N(2A)-Sn(1)-N(1) 90.30°; O(1)-Sn(1)-N(1) 93.36°] suggest the absence of significant *sp*-hybridisation at tin.

The Sn–O and Sn–N bond lengths within the eight-membered ring [Sn(1)-O(2) 2.1491(14), Sn(1)-N(2) 2.2751(19), and Sn(2)-O(2) 2.1434(15), Sn(2)-N(4) 2.2590(19) Å] are shorter than the range expected for simple Sn ← O and Sn ← N Lewis acid–base complexes [9,51,81–83]. Although the pyridine rings are stacked in the crystal lattice in an antiparallel-displaced

arrangement, the inter-ring distance ($>4 \text{ \AA}$) is greater than that expected for any significant electronic interaction (i.e., 3.4 \AA) [84].

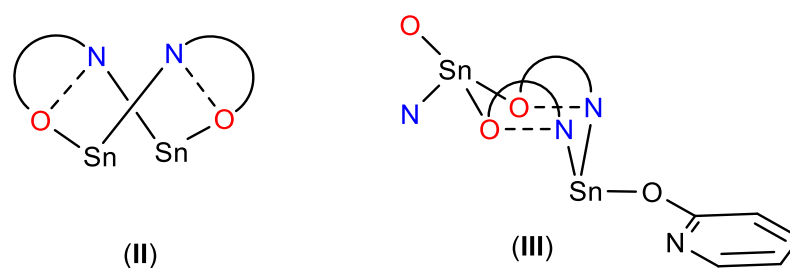
Furthermore, in each Sn-containing eight-membered ring, the core of the molecule adopts a chair-like ring conformation similar to that observed in the pyridine-selenolate complex $[\text{Sn}_2\{\mu\text{-}\eta^2\text{Se-2-C}_5\text{H}_4\text{N}\}_2\{\text{SeC}_5\text{H}_4\text{N}\}_2]$ [85]. While Sn(II) oxypyridinato complexes such as **1** have not, to the best of our knowledge, been previously reported, the core structure of **1** is reminiscent of Sn(II) carboxylate complexes $[\{\text{Sn}(\text{NR}_2)(\mu\text{-}\eta^2\text{-O}_2\text{CAR})_2\}]$ (Ar = *m*-terphenyl) [86]. As the bridging ligand oxypyridinato is isolobal to a carboxylate ligand $[\text{O}_2\text{CR}]$, this comparison is unsurprising. Similarly, **1** is also reminiscent of the *bis*(trimethylsilyl)amido Sn(II) triflate $[\{\text{Sn}(\text{NR}_2)(\mu\text{-}\eta^2\text{-OTf})_2\}]$ complex, which also consists of an Sn-containing eight-membered heterocyclic ring [83]. However, unlike the triflate derivative, complex **1** is a discrete entity and shows no evidence of intermolecular $\text{Sn}\cdots\text{O}$ interactions between adjacent eight-membered rings. The puckering of the central $\{\text{Sn}_2\text{O}_2\text{C}_2\text{N}_2\}$ ring may be considered to be a result of the folding of the eight-membered ring along the two inter-ligand $\text{O}\cdots\text{N}$ vectors, such that it adopts a chair-like conformation (I) (Scheme 5). The extent of the folding (θ_{ring}) may be defined as the angle between the $\{\text{SnON}\}$ planes and the $\{\text{O}_2\text{N}_2\}$ plane. In the absence of steric interactions, the “ideal” folding angle (θ_{ring}) should be ca. 130° ; the fold angle in **1** is $\theta_{\text{ring}} = 129.14^\circ$. A similar bonding arrangement for the $\mu_2\text{-O,N}$ hydroxypyridine ligand is observed in the aluminium complex $[(^t\text{Bu})_2\text{Al}(\mu\text{-O-2-C}_5\text{H}_4\text{N})_2]$ [70].



Scheme 5. Schematic drawing showing the coordination of the {hp} ligand in complex **1**.

The molecular structure of **2** is shown in Figure 6 and comprises a series of three eight-membered *spiro*- $\text{Sn}_2\text{O}_2\text{C}_2\text{N}_2$ rings that link through the Sn centres to create a one-dimensional three-link chain; selected bond lengths and angles are given in Table 3. Compound **2** is tetrameric, containing four Sn atoms and eight oxypyridinato ligands with three different coordination modes; two {hp} ligands are observed in terminal positions coordinating to the two three-coordinate Sn(II) centres via the oxygen atom of the {hp} ligand. Two oxypyridinato ligands in the central eight-membered ring bridge two four-coordinate Sn(II) centres in a $\mu\text{-}\eta^2$ head-to-tail (HT) coordination mode. The four remaining oxypyridinato ligands bridge between the two four-coordinate Sn(II) centre in the central 8-membered ring and the two three-coordinate Sn(II) centres in a $\mu\text{-}\eta^2$ head-to-head (HH) coordination mode.

At the centre of complex **2** is a $\{\text{Sn}_2\text{O}_2\text{C}_2\text{N}_2\}$ ring comparable in coordination geometry to that observed in complex **1**; the central ring in complex **2** can be considered to be in a boat-like conformation (II) (Scheme 6), resulting from folding along $\text{Sn}\cdots\text{O}$ vectors such that the two pyridine rings tend towards co-planarity, with an angle between the $\{\text{SnONC}_5\}$ planes of 35.36° and an inter-ring distance of $3.760(2) \text{ \AA}$. As a result of this puckering, the $\text{Sn}\cdots\text{Sn}$ distance in the inner ring is marginally reduced to 4.082 \AA (*cf.* 4.468 \AA in **1**).



Scheme 6. Schematic drawing showing the coordination of the {hp} ligands in complex 2.

Both Sn(II) centres in this central ring are four-coordinate, and may be considered to be the spiro atoms linking the three eight-membered {SnN₂C₂O₂Sn} rings together. While the two Sn(II) centres are four-coordinate, their geometry may be regarded as either distorted trigonal bipyramidal with a stereo-active lone pair of electrons or disphenoidal.

As noted above, the two outer {SnN₂C₂O₂Sn} rings are different to the central ring with the oxypyridinato ligands bridging the two Sn(II) centres in the outer rings in head-to-head bridging modes. The puckering of the “outer” Sn₂O₂C₂N₂ rings may be considered to be chair-like (III) (Scheme 6), resulting from the folding of the eight-membered ring along the two inter-ligand O···N vectors; θ_{ring} angle between {SnO₂} plane/{O₂N₂} plane = 39.91(5)°, and between {O₂N₂} plane/{SnN₂} plane = 97.92(5)°, thus resulting in a solid-state arrangement, such that the three-coordinate Sn(II) centres are folded under the {O₂N₂} plane (see (III) in Scheme 6).

The Sn–O and Sn–N bond lengths within both the three eight-membered rings and the exo-Sn–O bonds are within expected ranges for these complexes. Similarly, bond lengths and bond angles within the oxypyridinato ligands are all similar and within parameters observed in related complexes (*vide supra*).

While for complex 1 there are no comparable mono thio- or seleno-pyridinato complexes with which the coordination chemistry of oxy-pyridinato {hp} ligand can be compared, the homoleptic *bis*-thio and *bis*-seleno- complexes, [Sn{S-C₅NH₄}₂] [87] and [Sn{Se-C₅NH₄}₂] [85] are known, and display different structural chemistry to their oxygen-containing cousin, 2. Similarly, the homoleptic lead(II) 3,5-dinitro-2-pyridonate complex possesses a polymeric 1D solid-state structure, consisting of a {Pb₂O₂} core [73].

As noted above, during our investigation into the synthesis of complex 2, crystals of a second product were isolated from the reaction liquors. The single-crystal X-ray analysis of these crystals revealed the product to be the Sn(II) oxo cluster, [(Sn₆(μ₃-O)₆(μ-OC₅H₅N)₂(OC₅H₄N)₂):2{Sn(κ²ON-OC₅H₄N)₂}] (3), which is composed of a central {Sn₆O₆} core supported by four {hp} ligands, two of which are coordinated in *N,O*-μ-η² coordination mode, and two of which are terminal (Scheme 6). The cluster is further appended by the coordination of two [Sn{hp}₂] moieties, previously unobserved in this study, via a dative O←Sn interaction between two {μ₃-O} groups of the {Sn₆O₆} cluster and the Sn atoms of [Sn{hp}₂] units (Scheme 3).

While the principal {Sn₆O₆} core is comparable to other Sn(II) oxo-alkoxide systems [88], to the best of our knowledge, this is the first example of any such a cluster engaging in exo-coordinating to any metal centre via a dative M ← {μ₃-O} interaction, rather than an Sn(II) centre [89–92]. The molecular structure of complex 3 is shown in the supplementary information, along with selected bond lengths and bond angles.

The solid-state molecular structures of 4 and 5, as determined by single-crystal X-ray crystallography, are shown in Figure 7, with selected bond distances (Å) and bond angles (°) in Table 4. Complex 3 crystallises in orthorhombic space group *Pbcn* with half of the molecular complex in the asymmetric unit. Contrastingly, complex 5 crystallises in the triclinic space group *P-1*, with one full molecule in the unit cell alongside one whole molecule of disordered toluene.

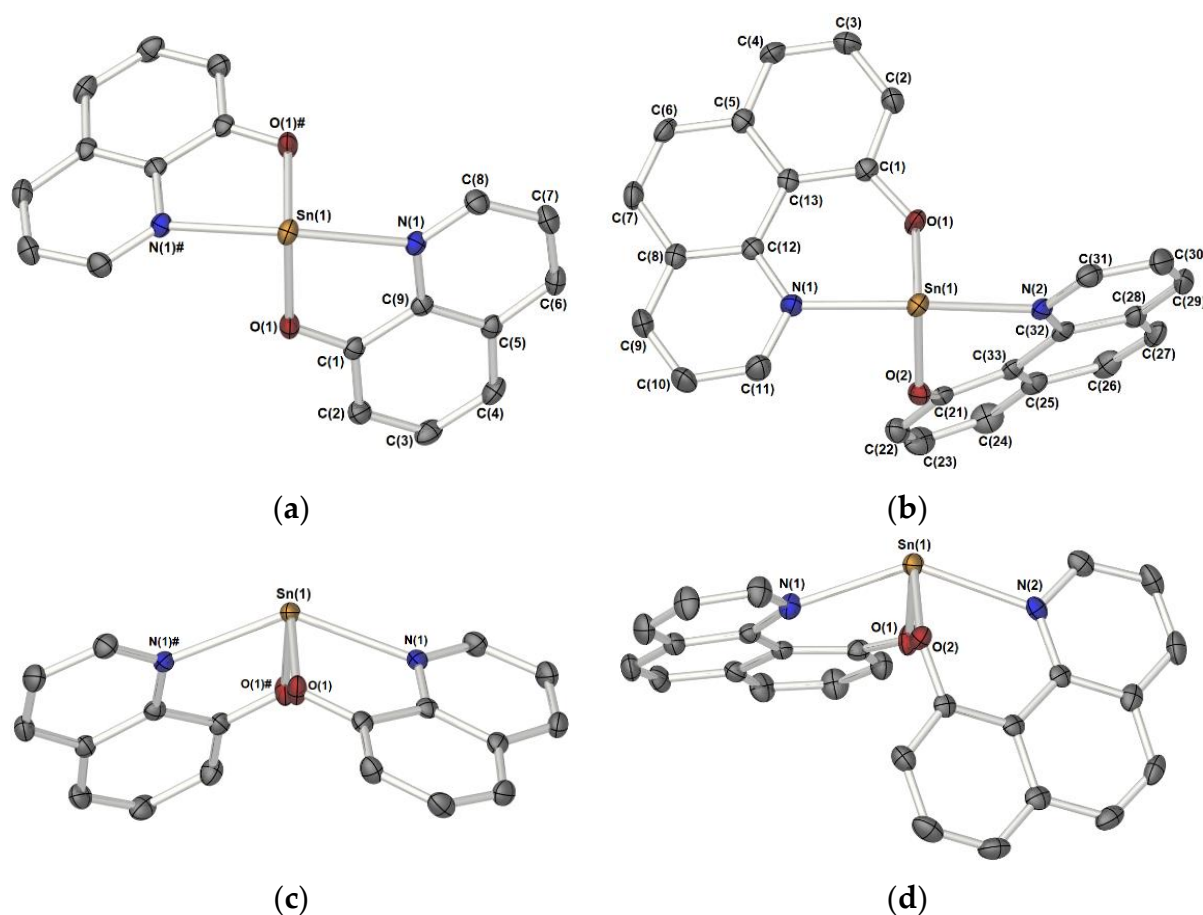


Figure 7. The molecular structure of **4** (a,c) and **5** (b,d). Thermal ellipsoids are shown at 50% probability. H-atoms are omitted for clarity. Solvent of crystallization (toluene) in **5** is omitted for clarity. Symmetry transformations used to generate equivalent atoms: #1 $3/2-X, Y, 1-Z$.

Table 4. Selected bond lengths (Å) and bond angles (°) for complexes **4** and **5**.

4		5	
Selected Bond Lengths (Å)			
Sn(1)-O(1)	2.0985(17)	Sn(1)-O(1)	2.0824(15)
		Sn(1)-O(2)	2.0779(17)
Sn(1)-N(1)	2.4014(19)	Sn(1)-N(1)	2.4140(19)
		Sn(1)-N(2)	2.4289(19)
O(1)-C(1)	1.326(3)	O(1)-C(1)	1.328(3)
		O(2)-C(21)	1.326(3)
Selected bond angles (°) ¹			
N(1)-Sn(1)-N(1)#	138.54(9)	N(1)-Sn(1)-N(2)	141.52(7)
O(1)-Sn(1)-O(1)#	98.23(10)	O(1)-Sn(1)-O(2)	97.33(7)

¹ # denotes symmetry generated atom (#: $3/2-X, Y, 1-Z$).

The solid-state structures of **4** and **5** are consistent with the spectroscopic data, suggesting the monomeric structures of the complexes in the solid-state are retained in solution. Both complexes have what may be described as “two-bladed propeller”-like geometry, with a C_2 axis lying on the bisectors of the N–Sn–N axis. Whilst **3** and **4** are both chiral, by virtue of their molecular C_2 symmetry, the enantiomers co-crystallise in non-centrosymmetric space groups.

Despite coordination numbers of four, in both **4** and **5**, analysis of the N–Sn–N and O–Sn–O bond angles about the Sn(II) centres suggests the Sn atoms adopt a pseudo trigonal

bipyramidal, or disphenoidal geometry, each with a stereoactive lone pair of electrons [4: $\tau = 0.67$, 5: $\tau = 0.74$] with the nitrogen atoms occupying the axial coordination sites and oxygen atoms the equatorial positions. The N–Sn–N bond angles increase from $\sim 138.5^\circ$ to 141.5° as the chelate ring is changed from 1,4- κ^2N,O , to 1,5- κ^2N,O coordination, respectively. The associated O–Sn–O angles [4: $98.224(17)^\circ$, 5: $97.331(14)^\circ$] are both close to 90° , suggesting that the Sn–O bonds are largely based around the Sn(II) *p*-orbitals. The 1,4- κ^2N,O and 1,5- κ^2N,O coordination of the ligands are associated with acute bite angles (N–Sn–O) of $73.23(2)^\circ$ for 4 and $74.76(3)/77.07(3)^\circ$ for 5 and induce a distortion of the axial vector (N–Sn–N) from linearity to angles of $138.56(2)^\circ$ and $141.52(5)^\circ$ for 4 and 5, respectively.

In complexes 4 and 5, the Sn–O distances (4: 2.0985(17) Å; 5: 2.0824(15) and 2.0779(17) Å) are slightly shorter than comparable Sn–O interactions in complexes 1 and 2. For 4, the Sn–O and Sn–N bond lengths are comparable to related systems (*vide supra*). Contrastingly, the Sn–N interactions in 4 and 5 (2.4014(19) Å and 2.4140(19)/2.4289(19) Å) are slightly longer than those observed in 1 and 2. However, both Sn–O and Sn–N bond lengths are in good agreement with the interatomic distances reported for comparable Sn(II) O–N chelate complexes (*vide supra*).

As noted previously, complex 4 possesses molecular C_2 symmetry. In contrast, one of the {hbq} ligands is folded along the inter-ligand O(1)⋯N(2) vectors, such that the three-rings of the {hbq} ligand are moved away from the second {hbq} ligand. A closer inspection of the intermolecular distances associated with complex 5 reveals both favourable π - π stacking interactions, between the {C(1)-N(1)} and {C(1)#-N(1)#} poly-aromatic rings, [$3.687(12)$ Å between the parallel planes defined by the atoms {C(1)-N(1)} and {C(1)#-N(1)#}, respectively], and C–H⋯ π interactions between adjacent molecules as shown in Figure 8, [$H(4)-(1)_{cent} = 2.658(12)$ Å and $H(6)-(2)_{cent} = 3.227(12)$ Å], which are presumably the origin of the observed distortion from molecular C_2 symmetry in the solid state. Interestingly, complex 5 appears to be one of a small number of structurally characterised examples of the {hbq} ligand coordinated to a metal centre, other than [Be{hbq}₂] [93] [Me₂Ga{hbq}] and [Me₂In{hbq}]₂ [94], as reported in the literature.

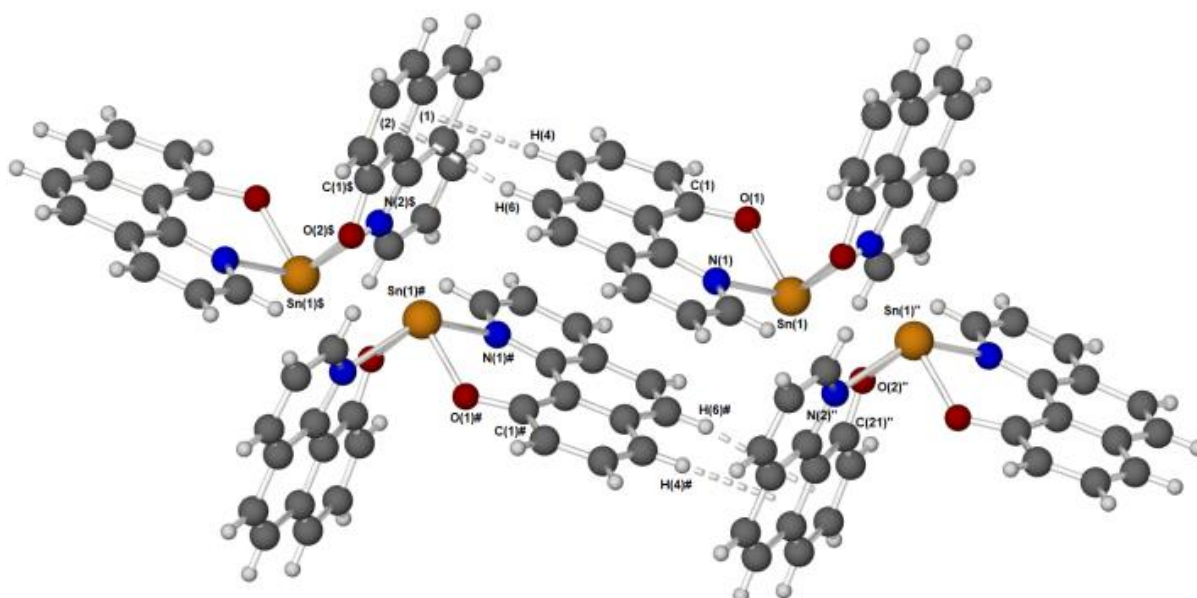


Figure 8. A representation of the H-Bonding and π - π stacking observed in the solid-state structure of 5. Bond lengths: $H(4)-(1)_{cent} = 2.658(12)$ Å and $H(6)-(2)_{cent} = 3.227(12)$ Å. Inter-plane distance: {C(1)-N(1)}/{C(1)#-N(1)#} = $3.687(12)$ Å. Symmetry transformations used to generate equivalent atoms: #1: X-1, 1+Y, -Z; #: X-1, 1+Y, Z; #'' X-1, 1+Y, Z.

4. Experimental Section

Experimental Details: ^1H , ^{13}C , and ^{119}Sn NMR spectra were recorded on Bruker Avance 300 or 500 MHz FT-NMR spectrometers, as appropriate, in saturated solutions at room temperature. Chemical shifts are expressed in ppm with respect to Me_4Si (^1H and ^{13}C) and SnMe_4 (^{119}Sn) in C_6D_6 . Elemental Analysis was performed externally by London Metropolitan University Elemental Analysis Service.

All reactions were carried out under an inert atmosphere using standard Schlenk techniques. The solvents were dried and degassed under an argon atmosphere over activated alumina columns using an Innovative Technology solvent purification system (SPS). The Sn(II) amide, $[\text{Sn}\{\text{N}(\text{SiMe}_3)_2\}_2]$, was prepared by the literature methods [95].

Synthesis of $[\text{Sn}(\mu\text{-}\kappa^2\text{ON-OC}_5\text{H}_4\text{N})(\text{N}(\text{SiMe}_3)_2)_2]$ (1): To a cooled solution of $[\text{Sn}\{\text{N}(\text{SiMe}_3)_2\}_2]$ (1 mmol, 0.44 g) in toluene (10 mL) a suspension of 2-hydroxypyridine (1 mmol, 0.10 g) in toluene (10 mL) was added and stirred for 2 hrs. The resulting solution gradually became yellow in colour. The reaction mixture was heated to near reflux and filtered through a Celite[®] pad (hot) to afford a clear pale-yellow filtrate. The removal of excess solvent under vacuum followed by storage at $-28\text{ }^\circ\text{C}$ yielded 0.20 g pale yellow microcrystals crystals (Yield = 54%). Elemental Analysis ($\text{C}_{11}\text{H}_{22}\text{N}_2\text{OSi}_2\text{Sn}$)₂ (expected): C 35.59% (35.40%), H 6.02% (5.94%), N 7.51% (7.51%). ^1H NMR (C_6D_6 , 500 MHz): δ 0.37 (s, 18H, $-\text{N}\{\text{SiMe}_3\}_2$), 6.19–6.23 (m, 1H, 5-CH), 6.47–6.50 (m, 1H, 3-CH), 6.94–6.99 (m, 1H, 4-CH), 7.97–8.01 (m, 1H, 6-CH). ^{13}C NMR (C_6D_6 , 125.7 MHz): δ 6.0 ($-\text{N}\{\text{SiMe}_3\}_2$), 114.0 (5-C), 116.6 (3-C), 142.2 (4-C), 142.6 (6-C), 170.0 (2-C). ^{119}Sn NMR (C_6D_6 , 186.5 MHz): δ -85 .

Synthesis of $[\text{Sn}_4(\mu\text{-}\kappa^2\text{ON-OC}_5\text{H}_4\text{N})_6(\kappa^1\text{O-OC}_5\text{H}_4\text{N})_2]$ (2): To a cooled solution of $[\text{Sn}\{\text{N}(\text{SiMe}_3)_2\}_2]$ (2 mmol, 0.88 g) in toluene (10 mL) a suspension of 2-Hydroxypyridine (4 mmol, 1.23 g) in toluene (10 mL) was added. A colourless precipitate was observed to form over time. The suspension was allowed to stir for 2 h before the precipitate was heated into solution. Filtration through a Celite[®] pad afforded a colourless filtrate. Slow cooling ($-28\text{ }^\circ\text{C}$) afforded 0.58 g of small starburst colourless crystals. (yield = 94%). Elemental Analysis ($\text{C}_{10}\text{H}_8\text{N}_2\text{O}_2\text{Sn}$)₄ (expected): C 38.7% (39.14%), H 2.85% (2.63%), N 9.11% (9.13%). ^1H NMR (C_6D_6 , 500 MHz): δ 5.98–6.05 (m, 1H, 5-CH), 6.54–6.61 (m, 1H, 3-CH), 6.88–6.95 (m, 1H, 4-CH), 7.58–7.67 (m, 1H, 6-CH). ^{13}C NMR (C_6D_6 , 125.7 MHz): δ 112.71 (5-C), 115.70 (3-C), 140.44 (4-C), 143.73 (6-C), 19.30 (2-C). ^{119}Sn NMR (C_6D_6 , 186.5 MHz): δ -526 .

Synthesis of $[\text{Sn}(\mu\text{-}\kappa^2\text{ON-OC}_9\text{H}_6\text{N})_2]$ (4): A suspension of 8-Hydroxyquinoline (4 mmol, 0.5806 g) in toluene (10 mL) was added, via cannula, to a cooled solution of $[\text{Sn}\{\text{N}(\text{SiMe}_3)_2\}_2]$ (2 mmol, 0.88 g) in toluene. A bright yellow precipitate was generated instantly. The suspension was allowed to stir for 2 h before the precipitate was heated into solution and filtered through a Celite[®] pad affording a yellow filtrate. Slow cooling ($-28\text{ }^\circ\text{C}$) afforded 0.62 g of large yellow crystals. (yield = 76%). Elemental Analysis $\text{C}_{18}\text{H}_{12}\text{N}_2\text{O}_2\text{Sn}$ (expected): C 53.27% (53.12%), H 3.02% (2.97%), N 6.85% (6.88%). ^1H NMR (C_6D_6 , 500 MHz): δ 8.32 (d, $J^3_{\text{H-H}} = 5\text{ Hz}$, 1H 2-CH) 7.45 (d, $J^3_{\text{H-H}} = 10\text{ Hz}$, 1H, 7-CH) 7.19 (dd, $J^3_{\text{H-H}} = 10\text{ Hz}$, $J^3_{\text{H-H}} = 10\text{ Hz}$, 1H, 3-CH), 7.10 (dd, $J^3_{\text{H-H}} = 10\text{ Hz}$, $J^3_{\text{H-H}} = 5\text{ Hz}$, 1H, 6-CH), 6.69 (d, $J^3_{\text{H-H}} = 10\text{ Hz}$, $J^3_{\text{H-H}} = 10\text{ Hz}$, 1H, 4-CH), 6.61 (dd, (dd, $J^3_{\text{H-H}} = 5\text{ Hz}$, $J^3_{\text{H-H}} = 5\text{ Hz}$, 1H, 5-CH). ^{13}C NMR (C_6D_6 , 125.7 MHz): δ 112.6 (4-C), 115.2 (6-C), 121.0 (5-C), 130.6 (3-C), 130.8 (8-C), 138.4 (7-C), 140.2 (9-C), 143.3 (2-C), 162.9 (1-C). ^{119}Sn NMR (C_6D_6 , 186.5 MHz): δ -386 .

Synthesis of $[\text{Sn}(\mu\text{-}\kappa^2\text{ON-OC}_{13}\text{H}_8\text{N})_2]$ (5): A suspension of 10-Hydroxybenzo[h]quinoline (4 mmol, 0.7810 g) in toluene (10 mL) was added, via cannula, to a cooled solution of $[\text{Sn}\{\text{N}(\text{SiMe}_3)_2\}_2]$ (2 mmol, 0.88 g) in toluene. A bright yellow precipitate was generated instantly. The suspension was stirred for 2 h before the precipitate was heated into solution and filtered through a Celite[®] pad affording a yellow filtrate. Slow cooling ($-28\text{ }^\circ\text{C}$) afforded 0.62 g of large yellow crystals. (yield = 85%). Elemental Analysis $\text{C}_{26}\text{H}_{16}\text{N}_2\text{O}_2\text{Sn}:\text{C}_7\text{H}_8$ (expected): C 65.97% (66.04%), H 4.11% (4.03%), N 4.65% (4.66%). ^1H NMR (C_6D_6 , 500 MHz): δ 6.67 (dd, $J^3_{\text{H-H}} = 10\text{ Hz}$, 5 Hz, 1H, CH), 6.83 (dd, $J^3_{\text{H-H}} = 5\text{ Hz}$, 2 Hz, 2H, CH), 6.91 (dd, $J^3_{\text{H-H}} = 10\text{ Hz}$, 10 Hz, 1H, CH), 6.99–7.03 (m 2H CH), 7.22 (d, $J^3_{\text{H-H}} = 2\text{ Hz}$, 1H, CH), 8.08 (dd, $J^3_{\text{H-H}} = 5\text{ Hz}$, 2 Hz, 1H, CH), 8.79 (dd, $J^3_{\text{H-H}} = 5\text{ Hz}$, 2 Hz,

1H, CH). ¹³C NMR (C₆D₆, 125.7 MHz): δ 116.9, 118.3, 120.0, 120.3, 120.7, 123.0, 125.6, 126.3, 126.7, 130.6, 145.0, 145.6, 169.3. ¹¹⁹Sn NMR (C₆D₆, 186.5 MHz): δ −542.

Single Crystal X-ray Diffraction Studies: Experimental details relating to the single-crystal X-ray crystallographic data for compounds 1–4 are summarized in Table S1 (ESI). The single-crystal X-ray crystallography data were collected at 150 K on RIGAKU Super-Nova Dual wavelength diffractometer equipped with an Oxford Cryostream, featuring a micro source with MoK α radiation ($\lambda = 0.71073 \text{ \AA}$) and Cu K α radiation ($\lambda = 1.5418 \text{ \AA}$). Crystals were isolated from an argon-filled Schlenk flask and immersed under oil before being mounted onto the diffractometer. The structures were solved by direct methods throughout and refined on F₂ data using the OLEX2 suite of programs [30]. All hydrogen atoms were included in idealized positions and refined using the riding model. Refinements were straightforward with no additional points that merit note. CCDC 2015978–2015982 contains the supplementary crystallographic data for this paper. These data can be obtained free of charge at www.ccdc.cam.ac.uk/conts/retrieving.html (accessed on 25 July 2022) [or from the Cambridge Crystallographic Data Centre, 12, Union Road, Cambridge CB2 1EZ, UK; Fax: + 44-1223/336-033; E-mail: deposit@ccdc.cam.ac.uk].

5. Conclusions

In recent years, 1,3-O,N, 1,4-O,N, and to a lesser extent 1,5-O,N chelate ligands based around the “basic” oxo-pyridinato system have been shown to play an important role as sterically and electronically tuneable ligands to a range of metal centres. The ambidentate nature of these tuneable ligands has allowed the stabilisation of metals spanning most of the periodic table. However, there is a paucity of main group metal examples bearing such ligands. Here, we describe an explorative investigation into the chemistry of these systems and highlight the array of reactive and novel bonding modes such versatile ligands display in a family of Sn(II) complexes bearing the pyridinato ligands oxopyridinato {hp} (1 and 2), quinolinato, {hq} (3) and oxybenzo[h]quinolinato {hbq} (4). The Sn(II) complexes bearing these ligands were synthesized and characterised in solution and in the solid state. In the case of the 1,3- κ^2 NO oxopyridinato systems, the ligand displays a diverse coordination geometry, mirroring some observations noted in transition metal chemistry. In contrast, the coordination chemistry of the quinolinato, {hq}, and oxybenzo[h]quinolinato {hbq} ligands display a much more limited variety in their bonding modes, with 3 and 4 displaying distorted trigonal bipyramidal geometries. To the best of our knowledge, complexes 1 and 2 are the first reported examples of Sn(II) centres supported by oxo-pyridinato ligands. In addition, complex 5 is a rare example of a coordination complex of the oxybenzo[h]quinolinato (5) ligands, and as such, one of only a small number from across the whole of the periodic table.

Supplementary Materials: The following supporting information can be downloaded at: <https://www.mdpi.com/article/10.3390/inorganics10090129/s1>, Figure S1: Two views of the molecular structure of complex 3; Table S1: Selected Bond lengths [\AA] for Complex 3; Table S2: Selected Bond angles [$^\circ$] for complex 3; Table S3: Crystal data and structure refinement for complexes 1–5.

Author Contributions: Conceptualization, A.L.J.; methodology, H.S.I.S.; Crystallographic analysis, A.L.J. and G.K.-K.; NMR Investigation, A.J.S.; writing—original draft preparation, A.L.J.; writing—review and editing, A.L.J. and A.J.S.; supervision, A.L.J.; project administration, A.L.J.; funding acquisition, A.L.J. All authors have read and agreed to the published version of the manuscript.

Funding: This research was funded by EPSRC, grant number EP/L0163541 and EP/G03768X/1.

Institutional Review Board Statement: Not applicable.

Informed Consent Statement: Not applicable.

Data Availability Statement: All the data reported in the study can be found in the supporting information and from the CCDC repository with accession numbers: 2015978–2015982.

Acknowledgments: We thank the EPSRC Doctoral Training Centre in Sustainable Chemical Technologies (CSCT) for a PhD studentship (H.S.I.S).

Conflicts of Interest: The authors declare no conflict of interest.

References

1. Lappert, M.; Protchenko, A.; Power, P.; Seeber, A. Subvalent Amides of Silicon and the Group 14 Metals. In *Metal Amide Chemistry*; John Wiley & Sons Ltd.: Hoboken, NJ, USA, 2008; pp. 263–326.
2. Mizuhata, Y.; Sasamori, T.; Tokitoh, N. Stable Heavier Carbene Analogues. *Chem. Rev.* **2009**, *109*, 3479–3511. [[CrossRef](#)] [[PubMed](#)]
3. Lee, V.Y.; Sekiguchi, A. *Organometallic Compounds of Low-Coordinate Si, Ge, Sn and Pb: From Phantom Species to Stable Compounds*; Wiley: Oxford, UK, 2010.
4. Dias, H.V.R.; Wang, Z. Germanium-Containing Heterobicyclic 10- π -Electron Ring Systems. Synthesis and Characterization of Neutral and Cationic Germanium(II) Derivatives of Aminotroponimines. *J. Am. Chem. Soc.* **1997**, *119*, 4650–4655. [[CrossRef](#)]
5. Akkari, A.; Byrne, J.J.; Saur, I.; Rima, G.; Gornitzka, H.; Barrau, J. Three coordinate divalent Group 14 element compounds with a β -diketiminate as supporting ligand L2MX [L2=PhNC(Me)CHC(Me)NPh, X = Cl, I; M = Ge, Sn]. *J. Organomet. Chem.* **2001**, *622*, 190–198. [[CrossRef](#)]
6. Sen, S.S.; Kritzler-Kosch, M.P.; Nagendran, S.; Roesky, H.W.; Beck, T.; Pal, A.; Herbst-Irmer, R. Synthesis of Monomeric Divalent Tin(II) Compounds with Terminal Chloride, Amide, and Triflate Substituents. *Eur. J. Inorg. Chem.* **2010**, *2010*, 5304–5311. [[CrossRef](#)]
7. Zaitsev, K.V.; Cherepakhin, V.S.; Churakov, A.V.; Peregudov, A.S.; Tarasevich, B.N.; Egorov, M.P.; Zaitseva, G.S.; Karlov, S.S. Extending the family of stable heavier carbenes: New tetrylenes based on N,N,O-ligands. *Inorg. Chim. Acta* **2016**, *443*, 91–100. [[CrossRef](#)]
8. Ahmet, I.Y.; Hill, M.S.; Raithby, P.R.; Johnson, A.L. Tin guanidinato complexes: Oxidative control of Sn, SnS, SnSe and SnTe thin film deposition. *Dalton Trans.* **2018**, *47*, 5031–5048. [[CrossRef](#)]
9. Parish, J.D.; Snook, M.W.; Johnson, A.L.; Kociok-Köhn, G. Synthesis, characterisation and thermal properties of Sn(ii) pyrrolide complexes. *Dalton Trans.* **2018**, *47*, 7721–7729. [[CrossRef](#)]
10. Holt, M.S.; Wilson, W.L.; Nelson, J.H. Transition metal-tin chemistry. *Chem. Rev.* **1989**, *89*, 11–49. [[CrossRef](#)]
11. Bartolin, J.M.; Kavara, A.; Kampf, J.; Banaszak Holl, M.M. Tin-Mediated CH Activation and Cross-Coupling in a Single Flask. *Organometallics* **2006**, *25*, 4738–4740. [[CrossRef](#)]
12. Summerscales, O.T.; Caputo, C.A.; Knapp, C.E.; Fettinger, J.C.; Power, P.P. The Role of Group 14 Element Hydrides in the Activation of C–H Bonds in Cyclic Olefins. *J. Am. Chem. Soc.* **2012**, *134*, 14595–14603. [[CrossRef](#)]
13. Lai, T.Y.; Fettinger, J.C.; Power, P.P. Facile C–H Bond Metathesis Mediated by a Stannylene. *J. Am. Chem. Soc.* **2018**, *140*, 5674–5677. [[CrossRef](#)] [[PubMed](#)]
14. Padělková, Z.; Nechaev, M.S.; Lyčka, A.; Holubová, J.; Zevaco, T.A.; Růžička, A. Reactivity of C,N-Chelated Stannylene with Azobenzene. *Eur. J. Inorg. Chem.* **2009**, *2009*, 2058–2061. [[CrossRef](#)]
15. Mandal, S.K.; Roesky, H.W. Group 14 Hydrides with Low Valent Elements for Activation of Small Molecules. *Acc. Chem. Res.* **2011**, *45*, 298–307. [[CrossRef](#)]
16. Stewart, C.A.; Dickie, D.A.; Moasser, B.; Kemp, R.A. Reactions of CO₂ and related heteroallenes with CF₃-substituted aromatic silylamines of tin. *Polyhedron* **2012**, *32*, 14–23. [[CrossRef](#)]
17. Padělková, Z.; Švec, P.; Pejchal, V.; Růžička, A. Activation of E–Cl bonds (E = C, Si, Ge and Sn) by a C,N-chelated stannylene. *Dalton Trans.* **2013**, *42*, 7660–7671. [[CrossRef](#)] [[PubMed](#)]
18. Wildsmith, T.; Hill, M.S.; Johnson, A.L.; Kingsley, A.J.; Molloy, K.C. Exclusive formation of SnO by low temperature single-source AACVD. *Chem. Commun.* **2013**, *49*, 8773–8775. [[CrossRef](#)]
19. Chu, T.; Nikonov, G.I. Oxidative Addition and Reductive Elimination at Main-Group Element Centers. *Chem. Rev.* **2018**, *118*, 3608–3680. [[CrossRef](#)]
20. Hadlington, T.J.; Driess, M.; Jones, C. Low-valent group 14 element hydride chemistry: Towards catalysis. *Chem. Soc. Rev.* **2018**, *47*, 4176–4197. [[CrossRef](#)]
21. Dove, A.P.; Gibson, V.C.; Marshall, E.L.; White, A.J.P.; Williams, D.J. A well defined tin(ii) initiator for the living polymerisation of lactide. *Chem. Commun.* **2001**, *2001*, 283–284. [[CrossRef](#)]
22. Kim, S.B.; Sinsersuksakul, P.; Hock, A.S.; Pike, R.D.; Gordon, R.G. Synthesis of N-Heterocyclic Stannylene (Sn(II)) and Germylene (Ge(II)) and a Sn(II) Amidinate and Their Application as Precursors for Atomic Layer Deposition. *Chem. Mater.* **2014**, *26*, 3065–3073. [[CrossRef](#)]
23. Catherall, A.L.; Harris, S.; Hill, M.S.; Johnson, A.L.; Mahon, M.F. Deposition of SnS Thin Films from Sn(II) Thioamidate Precursors. *Cryst. Growth Des.* **2017**, *17*, 5544–5551. [[CrossRef](#)]
24. Kim, H.-S.; Jung, E.A.; Han, S.H.; Han, J.H.; Park, B.K.; Kim, C.G.; Chung, T.-M. Germanium Compounds Containing Ge=E Double Bonds (E = S, Se, Te) as Single-Source Precursors for Germanium Chalcogenide Materials. *Inorg. Chem.* **2017**, *56*, 4084–4092. [[CrossRef](#)]
25. Ahmet, I.Y.; Thompson, J.R.; Johnson, A.L. Oxidative Addition to Sn(II) Guanidinate Complexes: Precursors to Tin(II) Chalcogenide Nanocrystals. *Eur. J. Inorg. Chem.* **2018**, *2018*, 1670–1678. [[CrossRef](#)]

26. Park, J.-H.; Kang, S.G.; Lee, Y.K.; Chung, T.-M.; Park, B.K.; Kim, C.G. Tin(II) Aminothiolate and Tin(IV) Aminothiolate Selenide Compounds as Single-Source Precursors for Tin Chalcogenide Materials. *Inorg. Chem.* **2020**, *59*, 3513–3517. [[CrossRef](#)]
27. Foley, S.R.; Yap, G.P.A.; Richeson, D.S. Oxidative addition to M(II) (M = Ge, Sn) amidinate complexes: Routes to group 14 chalcogenolates with hypervalent coordination environments. *J. Chem. Soc. Dalton Trans.* **2000**, *2000*, 1663–1668. [[CrossRef](#)]
28. Nimitsiriwat, N.; Gibson, V.C.; Marshall, E.L.; White, A.J.P.; Dale, S.H.; Elsegood, M.R.J. Tert-butylamidinate tin(ii) complexes: High activity, single-site initiators for the controlled production of polylactide. *Dalton Trans.* **2007**, *2007*, 4464–4471. [[CrossRef](#)]
29. Chlupatý, T.; Růžičková, Z.; Horáček, M.; Alonso, M.; De Proft, F.; Kampová, H.; Brus, J.; Růžička, A. Oxidative Additions of Homoleptic Tin(II) Amidinate. *Organometallics* **2015**, *34*, 606–615. [[CrossRef](#)]
30. Chlupatý, T.; Padělková, Z.; DeProft, F.; Willem, R.; Růžička, A. Addition of Lappert's Stannylenes to Carbodiimides, Providing a New Class of Tin(II) Guanidates. *Organometallics* **2012**, *31*, 2203–2211. [[CrossRef](#)]
31. Barman, M.K.; Baishya, A.; Peddara, T.; Nembenna, S. Guanidinate stabilized germanium(II) and tin(II) amide complexes and their catalytic activity for aryl isocyanate cyclization. *J. Organomet. Chem.* **2014**, *772–773*, 265–270. [[CrossRef](#)]
32. Chlupatý, T.; Růžičková, Z.; Horáček, M.; Merna, J.; Alonso, M.; De Proft, F.; Růžička, A. Reactivity of Tin(II) Guanidinate with 1,2- and 1,3-Diones: Oxidative Cycloaddition or Ligand Substitution? *Organometallics* **2014**, *34*, 2202–2211. [[CrossRef](#)]
33. Ungpittagul, T.; Wongmahasirikun, P.; Phomphrai, K. Synthesis and characterization of guanidinate tin(ii) complexes for ring-opening polymerization of cyclic esters. *Dalton Trans.* **2020**, *49*, 8460–8471. [[CrossRef](#)] [[PubMed](#)]
34. Dove, A.P.; Gibson, V.C.; Marshall, E.L.; Rzepa, H.S.; White, A.J.P.; Williams, D.J. Synthetic, Structural, Mechanistic, and Computational Studies on Single-Site β -Diketimate Tin(II) Initiators for the Polymerization of ϵ -CLA. *J. Am. Chem. Soc.* **2006**, *128*, 9834–9843. [[CrossRef](#)] [[PubMed](#)]
35. Jana, A.; Roesky, H.W.; Schulzke, C. Hydrostannylation of Ketones and Alkynes with $LSnH$ [L = HC(CMeNAr)₂, Ar = 2,6-iPr₂C₆H₃]. *Inorg. Chem.* **2009**, *48*, 9543–9548. [[CrossRef](#)] [[PubMed](#)]
36. Jana, A.; Objartel, I.; Roesky, H.W.; Stalke, D. Reaction of β -diketimate tin(ii) dimethylamide $LSnNMe_2$ [L = HC(CMeNAr)₂; Ar = 2,6-iPr₂C₆H₃] with ketones and alkynes. *Dalton Trans.* **2010**, *39*, 4647–4650. [[CrossRef](#)] [[PubMed](#)]
37. Harris, L.A.M.; Coles, M.P.; Fulton, J.R. Synthesis and reactivity of tin amide complexes. *Inorg. Chim. Acta* **2011**, *369*, 97–102. [[CrossRef](#)]
38. Taylor, M.J.; Saunders, A.J.; Coles, M.P.; Fulton, J.R. Low-Coordinate Tin and Lead Cations. *Organometallics* **2011**, *30*, 1334–1339. [[CrossRef](#)]
39. Harris, L.A.M.; Tam, E.C.Y.; Coles, M.P.; Fulton, J.R. Lead and tin β -diketimate amido/anilido complexes: Competitive nucleophilic reactivity at the β -diketimate γ -carbon. *Dalton Trans.* **2014**, *43*, 13803–13814. [[CrossRef](#)]
40. Zemlyansky, N.N.; Borisova, I.V.; Kuznetsova, M.G.; Khrustalev, V.N.; Ustynyuk, Y.A.; Nechaev, M.S.; Lunin, V.V.; Barrau, J.; Rima, G. New stable germylenes, stannylenes, and related compounds. 1. Stable germanium(II) and tin(II) compounds $M(OCH_2CH_2NMe_2)_2$ (M = Ge, Sn) with intramolecular coordination metal-nitrogen bonds. Synthesis and structure. *Organometallics* **2003**, *22*, 1675–1681. [[CrossRef](#)]
41. Khrustalev, V.N.; Portnyagin, I.A.; Zemlyansky, N.N.; Borisova, I.V.; Nechaev, M.S.; Ustynyuk, Y.A.; Antipin, M.Y.; Lunin, V. New stable germylenes, stannylenes, and related compounds 6. Heteroleptic germanium(II) and tin(II) compounds [(SiMe₃)₂N-E-14-OCH(2)CH(2)NMe₂]_n (E-14 = Ge, n = 1; Sn, n = 2): Synthesis and structure. *J. Organomet. Chem.* **2005**, *690*, 1172–1177. [[CrossRef](#)]
42. Khrustalev, V.N.; Portnyagin, I.A.; Zemlyansky, N.N.; Borisova, I.V.; Ustynyuk, Y.A.; Antipin, M.Y. New stable germylenes, stannylenes, and related compounds. 5. Germanium(II) and tin(II) azides [N-3-E-14-OCH₂CH₂NMe₂]₂ (E-14 = Ge, Sn): Synthesis and structure. *J. Organomet. Chem.* **2005**, *690*, 1056–1062. [[CrossRef](#)]
43. Hollingsworth, N.; Horley, G.A.; Mazhar, M.; Mahon, M.F.; Molloy, K.C.; Haycock, P.W.; Myers, C.P.; Critchlow, G.W. Tin(II) aminoalkoxides and heterobimetallic derivatives: The structures of Sn₆(O)₄(dmae)₄, Sn₆(O)₄(OEt)₄ and [Sn(dmae)₂Cd(acac)₂]₂. *Appl. Organomet. Chem.* **2006**, *20*, 687–695. [[CrossRef](#)]
44. Khrustalev, V.N.; Glukhov, I.V.; Borisova, I.V.; Zemlyansky, N.N. New stable germylenes, stannylenes, and related compounds. 8. Amidogermanium(II) and -tin(II) chlorides R₂N-E-14-Cl (E-14 = Ge, R = Et; E-14 = Sn, R = Me) revealing new structural motifs. *Appl. Organomet. Chem.* **2007**, *21*, 551–556. [[CrossRef](#)]
45. Khrustalev, V.N.; Zemlyansky, N.N.; Borisova, I.V.; Kuznetsova, M.G.; Krut'ko, E.B.; Antipin, M.Y. New stable germylenes, stannylenes, and related compounds 7.* Synthesis and structures of compounds. *Russ. Chem. Bull.* **2007**, *56*, 267–270. [[CrossRef](#)]
46. Aysin, R.R.; Leites, L.A.; Bukalov, S.S.; Khrustalev, V.N.; Borisova, I.V.; Zemlyanskii, N.N.; Smirnov, A.Y.; Nechaev, M.S. Vibrational spectra and structural features of carbene analogs El(II)(OCH₂CH₂NMe₂)₂ and ClEl(II)OCH(2)CH(2)NMe(2) (El(II) = Ge, Sn, Pb). *Russ. Chem. Bull.* **2011**, *60*, 69–80. [[CrossRef](#)]
47. Han, J.H.; Chung, Y.J.; Park, B.K.; Kim, S.K.; Kim, H.-S.; Kim, C.G.; Chung, T.-M. Growth of p-Type Tin(II) Monoxide Thin Films by Atomic Layer Deposition from Bis(1-dimethylamino-2-methyl-2-propoxy)tin and H₂O. *Chem. Mater.* **2014**, *26*, 6088–6091. [[CrossRef](#)]
48. Han, S.H.; Jung, E.A.; Lee, J.H.; Kim, D.H.; Lee, G.Y.; Park, B.K.; Kim, C.G.; Son, S.U.; Chung, T.M. Synthesis and Structure of Novel Tin Complexes Containing Aminoalkoxide Ligands. *ChemistrySelect* **2018**, *3*, 7836–7839. [[CrossRef](#)]
49. Wang, L.; Kefalidis, C.E.; Roisnel, T.; Sinbandhit, S.; Maron, L.; Carpentier, J.-F.; Sarazin, Y. Structure vs. ¹¹⁹Sn NMR Chemical Shift in Three-Coordinated Tin(II) Complexes: Experimental Data and Predictive DFT Computations. *Organometallics* **2014**, *34*, 2139–2150. [[CrossRef](#)]

50. Alvarez-Rodriguez, L.; Cabeza, J.A.; Garcia-Alvarez, P.; Polo, D. Organic Amides as Suitable Precursors to Stabilize Stannylenes. *Organometallics* **2013**, *32*, 3557–3561. [[CrossRef](#)]
51. Nimitsiriwat, N.; Gibson, V.C.; Marshall, E.L.; Elsegood, M.R.J. The Reversible Amination of Tin(II)-Ligated Imines: Latent Initiators for the Polymerization of ϵ -CL. *Inorg. Chim. Acta* **2008**, *47*, 5417–5424. [[CrossRef](#)]
52. Nimitsiriwat, N.; Gibson, V.C.; Marshall, E.L.; Elsegood, M.R.J. Bidentate salicylaldiminato tin(II) complexes and their use as lactide polymerisation initiators. *Dalton Trans.* **2009**, *2009*, 3710–3715. [[CrossRef](#)]
53. Piromjitpong, P.; Ratanapanee, P.; Thumrongpatanaraks, W.; Kongsaree, P.; Phomphrai, K. Synthesis of cyclic polylactide catalysed by bis(salicylaldiminato)tin(II) complexes. *Dalton Trans.* **2012**, *41*, 12704–12710. [[CrossRef](#)] [[PubMed](#)]
54. Kao, H.-M.; Ho, S.-M.; Chen, I.C.; Kuo, P.-C.; Lin, C.-Y.; Tu, C.-Y.; Hu, C.-H.; Huang, J.-H.; Lee, G.-H. Synthesis and structures of three, four, and six-coordinate monomeric tin(II) and tin(IV) compounds containing η^2 -ketiminate ligands. *Inorg. Chim. Acta* **2008**, *361*, 2792–2798. [[CrossRef](#)]
55. Morrison, J.S.; Haendler, H.M. Some reactions of tin(II) chloride in nonaqueous solution. *J. Inorg. Nucl. Chem.* **1967**, *29*, 393–400. [[CrossRef](#)]
56. Sister, M.A.D.; Brother, C.C. Moessbauer and infrared spectra of some tin(II) complexes. *Inorg. Chim. Acta* **1969**, *3*, 169–173. [[CrossRef](#)]
57. Bhide, S.N.; Umopathy, P.; Sen, D.N. Oxidative addition reactions of tin(II) oxinates. *J. Indian Chem. Soc.* **1977**, *54*, 851–856.
58. Bhide, S.N.; Umopathy, P.; Gupta, M.P.; Sen, D.N. Tin-119 Moessbauer spectral studies in organotin(IV) and tin(II) substituted oxinates. *J. Inorg. Nucl. Chem.* **1978**, *40*, 1003–1007. [[CrossRef](#)]
59. Umopathy, P.; Badrinarayanan, S.; Sinha, A.P.B. An ESCA study of tin(IV) and tin(II) chelates with substituted 8-quinolins. *J. Electron Spectrosc. Relat. Phenom.* **1983**, *28*, 261–266. [[CrossRef](#)]
60. Uddin, M.J.; Islam, S.; Islam, M.A.; Begum, F.; Haider, S.Z. Synthesis, characterization and antimicrobial properties of some heavy metal oxinates. *J. Bangladesh Chem. Soc.* **1995**, *8*, 7–16.
61. Kitamura, C.; Maeda, N.; Kamada, N.; Ouchi, M.; Yoneda, A. Synthesis of 2-(substituted methyl)quinolin-8-ols and their complexation with Sn(II). *J. Chem. Soc. Perkin Trans. 1* **2000**, *2000*, 781–785. [[CrossRef](#)]
62. El-Sonbati, A.Z.; El-Bindary, A.A. Stereochemistry of new nitrogen containing aldehydes. V. Novel synthesis and spectroscopic studies of some quinoline Schiff bases complexes. *Pol. J. Chem.* **2000**, *74*, 621–630.
63. Yoneda, A.; Ohfuchi, S.; Hoshimoto, A.; Kitamura, C. Synthesis and characterization of 2-vinylene-8-quinolins using the Wittig reaction. *Kenkyu Hokoku Himeji Kogyo Daigaku Kogakubu* **2002**, *54*, 60–67.
64. Kitamura, C.; Yoneda, A.; Sugiura, K.; Sakata, Y. Bis(2-methyl-8-quinolinolato-N,O)tin(II). *Acta Crystallogr. Sect. C Cryst. Struct. Commun.* **1999**, *55*, 876–878. [[CrossRef](#)]
65. Rawson, J.M.; Winpenny, R.E.P. The coordination chemistry of 2-pyridone and its derivatives. *Coord. Chem. Rev.* **1995**, *139*, 313–374. [[CrossRef](#)]
66. Parsons, S.; Winpenny, R.E.P. Structural Chemistry of Pyridonate Complexes of Late 3d-Metals. *Acc. Chem. Res.* **1997**, *30*, 89–95. [[CrossRef](#)]
67. Albrecht, M.; Fiege, M.; Osetska, O. 8-Hydroxyquinolines in metallosupramolecular chemistry. *Coord. Chem. Rev.* **2008**, *252*, 812–824. [[CrossRef](#)]
68. Dolomanov, O.V.; Bourhis, L.J.; Gildea, R.J.; Howard, J.A.K.; Puschmann, H. OLEX2: A complete structure solution, refinement and analysis program. *J. Appl. Crystallogr.* **2009**, *42*, 339–341. [[CrossRef](#)]
69. Drover, M.W.; Love, J.A.; Schafer, L.L. 1,3-N,O-Complexes of late transition metals. Ligands with flexible bonding modes and reaction profiles. *Chem. Soc. Rev.* **2017**, *46*, 2913–2940. [[CrossRef](#)]
70. Francis, J.A.; Bott, S.G.; Barron, A.R. Aluminium compounds containing bidentate ligands: Chelate ring size and rigid conformation effects. *J. Chem. Soc. Dalton Trans.* **1998**, *19*, 3305–3310. [[CrossRef](#)]
71. Bashall, A.; Beswick, M.A.; Feeder, N.; Hopkins, A.D.; Kidd, S.J.; McPartlin, M.; Raithby, P.R.; Wright, D.S. Reactions of the spiro monoanion $[(\text{Me}_2\text{N})\text{Sb}(\mu\text{-NCy})_2]_2\text{Sb}^-$ with alcohols and thiols (REH; E = O or S); syntheses of nido- $[\text{Sb}_3(\mu\text{-NCy})_3(\mu_3\text{-NCy})(\text{ER})_2]$ anions and the unique antimony(III) imido cubane $[(2\text{-NC}_5\text{H}_4\text{O})\text{Sb}(\mu_3\text{-NCy})]_4$ (Cy = cyclohexyl). *J. Chem. Soc. Dalton Trans.* **2000**, *12*, 1841–1847. [[CrossRef](#)]
72. Bickley, J.F.; Bond, A.D.; García, F.; Jantos, K.; Lawson, G.T.; McPartlin, M.; Steiner, A.; Wright, D.S. Syntheses and structures of the cubanes $[\text{PhOSb}(\mu_3\text{-NCy})]_4$ and $[\text{pyOBi}(\mu_3\text{-NCy})]_4$ (Cy = cyclohexyl, py = 2-pyridyl). *J. Chem. Soc. Dalton Trans.* **2002**, *24*, 4629–4633. [[CrossRef](#)]
73. She, J.-B.; Zhang, G.-F.; Zhao, F.-Q.; Lei, Z.-L.; Fan, X.-Z. The first two structurally characterized energetic catalysts derived from dinitropyridone. *Struct. Chem.* **2007**, *18*, 373–378. [[CrossRef](#)]
74. Sunderland, T.L.; Berry, J.F. The first bismuth(II)–rhodium(II) oxyppyridinate paddlewheel complexes: Synthesis and structural characterization. *J. Coord. Chem.* **2016**, *69*, 1949–1956. [[CrossRef](#)]
75. Brewster, T.P.; Nguyen, T.H.; Li, Z.; Eckenhoff, W.T.; Schley, N.D.; DeYonker, N.J. Synthesis and Characterization of Heterobimetallic Iridium–Aluminum and Rhodium–Aluminum Complexes. *Inorg. Chem.* **2018**, *57*, 1148–1157. [[CrossRef](#)] [[PubMed](#)]
76. Neufeld, R.; Stalke, D. Accurate molecular weight determination of small molecules via DOSY-NMR by using external calibration curves with normalized diffusion coefficients. *Chem. Sci.* **2015**, *6*, 3354–3364. [[CrossRef](#)] [[PubMed](#)]
77. Bachmann, S.; Gernert, B.; Stalke, D. Solution structures of alkali metal cyclopentadienides in THF estimated by ECC-DOSY NMR-spectroscopy (incl. software). *Chem. Commun.* **2016**, *52*, 12861–12864. [[CrossRef](#)]

78. Kreyenschmidt, A.-K.; Bachmann, S.; Niklas, T.; Stalke, D. Molecular Weight Estimation of Molecules Incorporating Heavier Elements from van-der-Waals Corrected ECC-DOSY. *ChemistrySelect* **2017**, *2*, 6957–6960. [[CrossRef](#)]
79. Chisholm, M.H.; Clark, D.L.; Hampden-Smith, M.J. Hexaisopropoxyditungsten and dodecaisopropoxytetratungsten: W₂(O-i-Pr)₆ and W₄(O-i-Pr)₁₂. 2. Studies of cluster dynamics and the equilibrium between the 12-electron cluster and two metal-metal triple bonds. A symmetry-allowed [π .s₂ + π .s₂] cycloaddition reaction and comparisons with the chemistry of cyclobutadiene. *J. Am. Chem. Soc.* **2002**, *111*, 574–586. [[CrossRef](#)]
80. Boyle, T.J.; Alam, T.M.; Rodriguez, M.A.; Zechmann, C.A. Hydrolysis of Tin(II) Neo-pentoxide: Syntheses, Characterization, and X-ray Structures of [Sn(ONep)₂]_∞, Sn₅(μ₃-O)₂(μ-ONep)₆, and Sn₆(μ₃-O)₄(μ-ONep)₄ Where ONep = OCH₂CMe₃. *Inorg. Chem.* **2002**, *41*, 2574–2582. [[CrossRef](#)]
81. Wang, L.; Kefalidis, C.E.; Sinbandhit, S.; Dorcet, V.; Carpentier, J.-F.; Maron, L.; Sarazin, Y. Heteroleptic Tin(II) Initiators for the Ring-Opening (Co)Polymerization of Lactide and Trimethylene Carbonate: Mechanistic Insights from Experiments and Computations. *Chem.—A Eur. J.* **2013**, *19*, 13463–13478. [[CrossRef](#)]
82. Wiederkehr, J.; Wölper, C.; Schulz, S. Synthesis, solid-state structures and reduction reactions of heteroleptic Ge(II) and Sn(II) β-ketoiminate complexes. *Z. Für Nat. B* **2017**, *72*, 813–820. [[CrossRef](#)]
83. Hitchcock, P.B.; Lappert, M.F.; Lawless, G.A.; de Lima, G.M.; Pierssens, L.J.M. Synthesis and structural characterisation of bis(trimethylsilyl)amidotin(II) triflate [{Sn(NR₂)-(μ-η²(2)-OTf(2))]_n (R = SiMe₃, -OTf = -OSO₂CF₃). *J. Organomet. Chem.* **2000**, *601*, 142–146. [[CrossRef](#)]
84. Yao, Z.-F.; Wang, J.-Y.; Pei, J. Control of π-π Stacking via Crystal Engineering in Organic Conjugated Small Molecule Crystals. *Cryst. Growth Des.* **2017**, *18*, 7–15. [[CrossRef](#)]
85. Cheng, Y.F.; Emge, T.J.; Brennan, J.G. Pyridineselenolate complexes of tin and lead: Sn(2-SeNC₅H₄)(₂), Sn(2-SeNC₅H₄)(₄), Pb(2-SeNC₅H₄)(₂), and Pb(3-Me(3)Si-2-SeNC₅H₃)(₂). Volatile CVD precursors to group IV group VI semiconductors. *Inorg. Chem.* **1996**, *35*, 342–346. [[CrossRef](#)] [[PubMed](#)]
86. Dickie, D.A.; Lee, P.T.K.; Labeodan, O.A.; Schatte, G.; Weinberg, N.; Lewis, A.R.; Bernard, G.M.; Wasylshen, R.E.; Clyburne, J.A.C. Flexible coordination of the carboxylate ligand in tin(ii) amides and a 1,3-diaza-2,4-distannacyclobutanediyl. *Dalton Trans.* **2007**, *27*, 2862–2869. [[CrossRef](#)] [[PubMed](#)]
87. Wächtler, E.; Gericke, R.; Kutter, S.; Brendler, E.; Wagler, J. Molecular structures of pyridinethiolato complexes of Sn(II), Sn(IV), Ge(IV), and Si(IV). *Main Group Metal. Chem.* **2013**, *36*, 181–191. [[CrossRef](#)]
88. Barbul, I.; Johnson, A.L.; Kociok-Köhn, G.; Molloy, K.C.; Silvestru, C.; Sudlow, A.L. The Reaction and Materials Chemistry of [Sn₆(O)₄(OSiMe₃)₄]: Chemical Vapour Deposition of Tin Oxide. *ChemPlusChem* **2013**, *78*, 866–874. [[CrossRef](#)]
89. Schiemenz, B.; Ettel, F.; Huttner, G.; Zsolnai, L. Metallorganische schutzgruppen für den aufbau ungewöhnlicher zinn-chalkogenkäfiverbindungen: Thio-stannat(II) Sn₃S₄– und “Zinnoxidhydrat” Sn₆(μ₃-OH)₄(μ₃-O)₄ als Liganden in RCp(CO)₂Mn-Komplexen. *J. Organomet. Chem.* **1993**, *458*, 159–166. [[CrossRef](#)]
90. Sita, L.R.; Xi, R.; Yap, G.P.A.; Liable-Sands, L.M.; Rheingold, A.L. High Yield Synthesis and Characterization of Sn₆(μ₃-O)₄(μ₃-OSiMe₃)₄: A Novel Main Group Cluster for the Support of Multiple Transition Metal Centers. *J. Am. Chem. Soc.* **1997**, *119*, 756–760. [[CrossRef](#)]
91. Kircher, P.; Huttner, G.; Zsolnai, L.; Driess, A. Partially Oxidized Zintl Ions? The Characterization of [(μ₃-OH)(μ₃-O)₃(OEt)₃[(CO)₅W]₇Sn₇]²⁻. *Angew. Chem. Int. Ed.* **1998**, *37*, 1666–1668. [[CrossRef](#)]
92. Mertens, L.; Leonhardt, C.; Rüffer, T.; Toma, A.; Silvestru, C.; Mehring, M. Heterobimetallic tin(II) oxido clusters of the type [{Sn 6 (μ₃-O) 4 (μ₃-OCH 2 R) 4 } {W(CO) 5 } 4] and [{Sn 5 (μ₃-O) 2 (μ-OCH 2 R) 4 (μ₃-OCH 2 R) 2} {Fe(CO) 4 } 2]. *J. Organomet. Chem.* **2016**, *821*, 206–213. [[CrossRef](#)]
93. Freidzon, A.Y.; Safonov, A.A.; Bagaturyants, A.A. Theoretical Study of the Spectral and Charge-Transport Parameters of an Electron-Transporting Material Bis(10-hydroxybenzo[h]quinolinato)beryllium (Bebq₂). *J. Phys. Chem. C* **2015**, *119*, 26817–26827. [[CrossRef](#)]
94. Wu, X.S.; Sun, H.S.; Pan, Y.; Chen, H.B.; Sun, X.Z. The reaction of metal trialkyls with benzo[H]quinolin-10-ol. *Chin. Chem. Lett.* **1999**, *10*, 875–878.
95. Fjeldberg, T.; Hope, H.k.; Lappert, M.F.; Power, P.P.; Thorne, A.J. Molecular structures of the main group 4 metal(II) bis(trimethylsilyl)-amides M[N(SiMe₃)₂]₂ in the crystal (X-ray) and vapour (gas-phase electron diffraction). *J. Chem. Soc. Chem. Commun.* **1983**, *11*, 639–641. [[CrossRef](#)]